

PAPER • OPEN ACCESS

Plasma density measurement by means of self-modulation of long electron bunches

To cite this article: G Loisch *et al* 2019 *Plasma Phys. Control. Fusion* **61** 045012

View the [article online](#) for updates and enhancements.



IOP | ebooks™

Bringing you innovative digital publishing with leading voices to create your essential collection of books in STEM research.

Start exploring the [collection](#) - download the first chapter of every title for free.

Plasma density measurement by means of self-modulation of long electron bunches

G Loisch¹ , G Asova^{1,2} , P Boonpornprasert¹ , Y Chen¹ , J Good¹ ,
M Gross¹ , H Huck¹, D Kalantaryan¹, M Krasilnikov¹ , O Lishilin¹ ,
D Melkumyan¹, A Oppelt¹ , H Qian¹ , Y Renier^{1,3}, F Stephan¹  and
Q Zhao^{1,4}

¹ DESY Zeuthen, Platanenallee 6, D-15738 Zeuthen, Germany

² INRNE, BAS, 1784 Sofia, Bulgaria

E-mail: gregor.loisch@desy.de

Received 19 October 2018, revised 8 January 2019

Accepted for publication 6 February 2019

Published 7 March 2019



Abstract

We present a new method to determine the electron density of a plasma by measuring the periodicity of modulations introduced to the longitudinal phase space of a relativistic particle bunch by the interaction with the plasma via the self-modulation instability. As the modulation is solely depending on the plasma density and the beam parameters, this method allows to determine the time-resolved density of a plasma at the position of beam passage, which is confirmed in particle-in-cell simulations. Densities in the range of $3.6 \times 10^{12} \text{ cm}^{-3}$ – $7.2 \times 10^{15} \text{ cm}^{-3}$ have been measured and the measurement accuracy is confirmed by comparison to spectroscopic plasma density measurements.

Keywords: plasma wakefield acceleration, self-modulation instability, plasma based acceleration, plasma density measurement

(Some figures may appear in colour only in the online journal)

1. Introduction

The electron density of a plasma is one of the key figures of merit for application of laboratory plasmas. Parameters like plasma frequency, collision rates and Debye length, which describe the physical behavior of the plasma, can be derived from it.

In recent years particle acceleration in plasma wakefields has become one of the major areas of application for laboratory plasma sources. In such schemes either a high power laser (laser wakefield acceleration (LWFA)) [1] or a relativistic, high brightness particle bunch (beam-driven

plasma wakefield acceleration (PWFA)) [2] displaces plasma electrons from their equilibrium positions in the plasma due to the ponderomotive force or space charge force, respectively. As for the length of the driver beam being shorter than the plasma wavelength λ_p and the reaction time of the plasma electrons being limited by λ_p/c , the interaction leaves behind an area of positive charge excess from the heavy and therefore slow plasma ions. An oscillation is then created by the returning plasma electrons overshooting their original positions. In the fields present between positive and negative charge excess regions, trailing particles can be accelerated. These acceleration schemes are particularly interesting for future particle accelerators as acceleration gradients on the order of 100 GV m^{-1} have been achieved in experiment [3–5], exceeding acceleration gradients of conventional acceleration techniques by orders of magnitude.

One of the main future challenges will be the provision of fine-tunable and stable accelerators, suitable for applications. To achieve this, the parameters of the driving beam as well as of the plasma medium have to be determined with high accuracy.

³ Present address: DPNC-Université de Genève, 1211 Geneva, Switzerland.

⁴ On leave from Institute of Modern Physics, 730000 Lanzhou, People's Republic of China.



Original content from this work may be used under the terms of the [Creative Commons Attribution 3.0 licence](https://creativecommons.org/licenses/by/3.0/). Any further distribution of this work must maintain attribution to the author(s) and the title of the work, journal citation and DOI.

Presently the main non-invasive measurement principles for determination of plasma densities are either spectroscopic [6, 7] or interferometric [8] measurements. Methods based on the former principle are easy to set up and can reach high space and time resolution. Methods based on the latter can achieve even higher resolution, are independent of plasma ion species but are much more complex to set up. Both share the drawback that the exact position of electron beam passage is unknown and even with highly time- and space-resolved preparatory density measurements the actual density at the beam position has to be inferred in a certain range. Furthermore, the plasma medium can be hard to access in the accelerator environment due to space and safety constraints.

We therefore present a new method to determine the plasma density at the position of beam passage in arbitrary ion species plasmas with accuracies compatible with conventional methods. This new method is based on the so called self-modulation instability (SMI), an instability a particle bunch with length on the order of or longer than the plasma wavelength undergoes while driving a plasma wakefield [9–14].

2. SMI-based density measurement principle

Particles in a bunch which has a length on the order of or longer than the plasma wavelength and which drives a wakefield in a plasma (e.g. due to a sharp rising edge at the bunch head) experience all phases of the driven wake. Even if the transverse forces are all focusing along the bunch at the entry into the plasma, differences in the focusing strength lead to inhomogeneous focusing of different bunch slices and to periodic focusing and defocusing. This self-amplifying mechanism is called the SMI and it finally results in the formation of a train of focused bunchlets on axis with defocused slices in between.

As the bunchlets are experiencing the focusing phases of the transverse wakefields, which are 90° phase-shifted to the longitudinal fields, the bunchlets are partially accelerated and partially decelerated. The relationship between position and energy of the bunch particles in direction of main motion is described by the longitudinal phase space (LPS) of the bunch. Energy changes due to the wakefield are imprinted onto the LPS of the bunch and due to the fixed phase relation between transverse and longitudinal wakefields show the same periodicity as the bunchlets.

The plasma density measurement method we propose is based on measuring this periodicity in the LPS modulations by subtracting the mean slice energy of a bunch that did not interact with a plasma from the mean slice energy of a bunch that underwent SMI. As the LPS includes all energy changes introduced to the bunch particles along the plasma, the method does not provide local density information along the plasma, as long as the plasma length is fixed. The periodicity is determined via Fourier-transformation of the energy modulations. Due to the separation between bunchlets being equal to one plasma oscillation period, the main contribution to the LPS modulation is assumed to arise at the plasma frequency.

Hence the frequency with the maximum signal in the Fourier spectrum is assumed to represent the plasma electron frequency $f_{pe} = c/\lambda_p$. The plasma density n_0 is calculated according to

$$n_0 = \frac{\pi f_{pe}^2 m_e}{e^2}, \quad (1)$$

where m_e is the electron mass and e the electron charge [15].

To measure the LPS of high brightness electron bunches a transverse deflecting structure (TDS) [16] in combination with a dipole spectrometer is usually used: bunch particles are deflected according to their experienced phase of the TDS radiofrequency (RF) voltage (i.e. longitudinal position in the bunch) in one transverse direction and dispersed according to their energies by the dipole in the orthogonal transverse direction. The transverse projection of the bunch on a subsequent measurement screen yields the bunch LPS information. Even though the periodicity of the bunchlets is already accessible (e.g. in the bunch current profile) when a TDS without dipole spectrometer is employed, the measurement of the energy modulation in the LPS has several significant practical advantages:

- a single period (or even less) can be analyzed
- the growth of the instability can be inferred from the LPS modulations
- the TDS chromaticity (i.e. change of deflection for different particle energies) can be deduced from the measurement.

In proton-driven PWFA, where bunch lengths are usually significantly longer and also much longer than the plasma wavelength, LPS measurements can be impractical due to the high rigidity of the highly relativistic beam. Bunch current profiles (i.e. bunchlet periodicity) can here e.g. be measured using a streak-camera [14] and therefore the above-mentioned drawbacks do only partially apply. It is assumed that the periodicity of bunchlets in a long train yields the same plasma density as the present method, whereas this will not be further discussed in the following.

SMI has already been experimentally demonstrated to occur both in electron [13] as well as in proton bunches [14]. The LPS of self-modulated electron bunches has been measured after interaction with the plasma and densities have been inferred from the period length by manual evaluation, to roughly assess the plasma density [13]. Nevertheless, no defined method has been proposed for the SMI-based measurement of the plasma density and no detailed investigation of the validity and the error of the measured densities has been presented. Furthermore, no comparison to established density measurements has been reported thus far.

In this article we evaluate the validity and applicability of the proposed LPS-based density measurement method for the parameter space of the Photoinjector Test facility at DESY, Zeuthen site (PITZ) [17].

3. Simulations

3D particle-in-cell (PIC) simulations have been performed with the quasi-static PWFA code HiPACE [18] to assess the accuracy of the SMI-based density measurement. For these simulations the following beam and plasma parameters, available at the PITZ facility, have been scanned [17, 19–21]:

- unperturbed plasma density n_0 : 10^{12} – 10^{16} cm $^{-3}$
- plasma length L_p : 100 mm
- bunch shape: flat-top
- mean bunch energy: 23 MeV
- bunch length: ca. 25 ps full width at half maximum (FWHM)
- current rise time (10–90%): (1–2) ps
- bunch charge: (100–1000) pC
- transverse size at plasma entrance $\sigma_{x/y}$: 0.1–0.5 mm (root mean square, rms).

The flat-top bunch shape has been chosen as it deviates least from ideal instability dynamics [11]. A small uncorrelated energy spread was shown to reduce the influence of the Hosing instability [22] with no reported or observed influence on the SMI development. The uncorrelated energy spread was therefore set to 5%. No correlated energy spread was introduced. A grid of $512 \times 256 \times 256$ cells has been used to simulate a box of $12 \times 1 \times 1$ mm 3 .

Figure 1 shows the evolution of a bunch undergoing SMI (a), (b), the evolution of the slice energy modulations (c) and the Fourier spectrum of the slice energy changes in the middle of the plasma (d). The modulation into bunchlets is clearly visible in figure 1(b). The bunchlets in figure 1(b) are formed at phases of focusing transverse fields. Due to the linear regime of the interaction and the consequent 90° phase offset between longitudinal and transverse fields this results in an energy change along every individual bunchlet with an overall sinusoidal energy modulation along the bunchlet train (figure 1(c)). After formation of the bunchlets, their wakefields add up towards the tail of the bunch, which can also be seen in figure 1(c), where slice energy changes are shown for three different positions along the 100 mm long plasma channel: while at the start of the instability the slice energy modulations are nearly homogeneous along the bunch (blue curve), they significantly grow towards the bunch tail in later stages (red and yellow curves), due to the resonant wakefield excitation by the formed train of bunchlets. This general behavior can be utilized to deduce the growth stage of the instability from the LPS modulations. The density, which would be determined experimentally from the modulations after the full plasma length is 1.5% lower than the simulated density. Nevertheless, after 50 mm propagation length, the density that corresponds to the highest peak deviates by 16.5%, the one of the second emerging peak by 7.3% from the actually simulated density, as shown in figure 1(d). This higher error is caused by the change of wakefield phase velocity during the evolution of the SMI [11]. Figure 1(c) illustrates this effect: while the first period of the slice energy modulation is mainly changing in amplitude from 50 to

75 mm of plasma interaction, the following periods are also changed in shape. The positions of the maxima in energy loss along the bunch are changing significantly towards the end of the plasma. To understand the development of the measurement accuracy, figure 2 shows the ratio between simulated measurement and actually simulated density along the plasma for two different probe bunches. While their charge is similar to the case depicted in figure 1, a different plasma density and two different initial transverse bunch sizes were simulated.

In both cases the measured density drops significantly due to the phase velocity change during the bunchlet formation. Nevertheless the onset of this drop happens much earlier in the plasma in the case of smaller transverse bunch size, which corresponds to a higher initial wakefield amplitude (due to higher space charge), i.e. stronger seed of the instability. In terms of instability growth lengths $L_{\text{growthSMI}}$ [11], the transition occurs in the same development phase (see figure 2, right plot). After this a step in the measured plasma density towards better accuracy takes place. This corresponds to the appearance of the second (right) peak in figure 1(d). The reason is assumed to be that for the bunched beam, the separation between bunchlets is again close to one plasma wavelength, whereas the positions of the bunchlets are slightly different from their positions at the beginning. Therefore a peak close to the actual density arises after build-up of the bunchlets, in addition to the peak that originates from the modulations imprinted on the LPS prior to the phase transition. While the second peak does not necessarily emerge at densities higher than the actually simulated (compare figure 2), the density was always found to be significantly closer to the simulated density. No clear pattern for the exact density relation was found in simulations at various beam/plasma parameters, though. The second drop in accuracy might be caused by the transverse offsets of the defocused bunch particles: particles that are too far off axis do not experience significant longitudinal fields and therefore do not change their energies anymore. As they are still considered in the LPS measurements, they distort the LPS modulation shape and influence the measurement result.

To assess the dependence of the measurement error on the development state of the SMI, the measurement result was simulated for various bunch/plasma configurations of the PITZ parameter space. Whereas qualitatively the results follow the examples in figure 2, no pattern emerged that generally describes the simulated measurement error dependence on e.g. the number of e -foldings/growth lengths of the SMI. In most cases a reduction of the measurement error is observed after the formation of the bunchlets, i.e. after the phase velocity transition, due to the appearance of a second signature in the Fourier spectrum. Therefore the measurement accuracy is mostly optimal at very early stages (<10 growth lengths) or between 15 and 20 growth lengths. Measurements should therefore be done in these regimes by adjusting the bunch parameters to the expected plasma parameters, which might also be done iteratively.

The maximum deviation of the measured and the actually simulated plasma density at the end of the plasma in PITZ

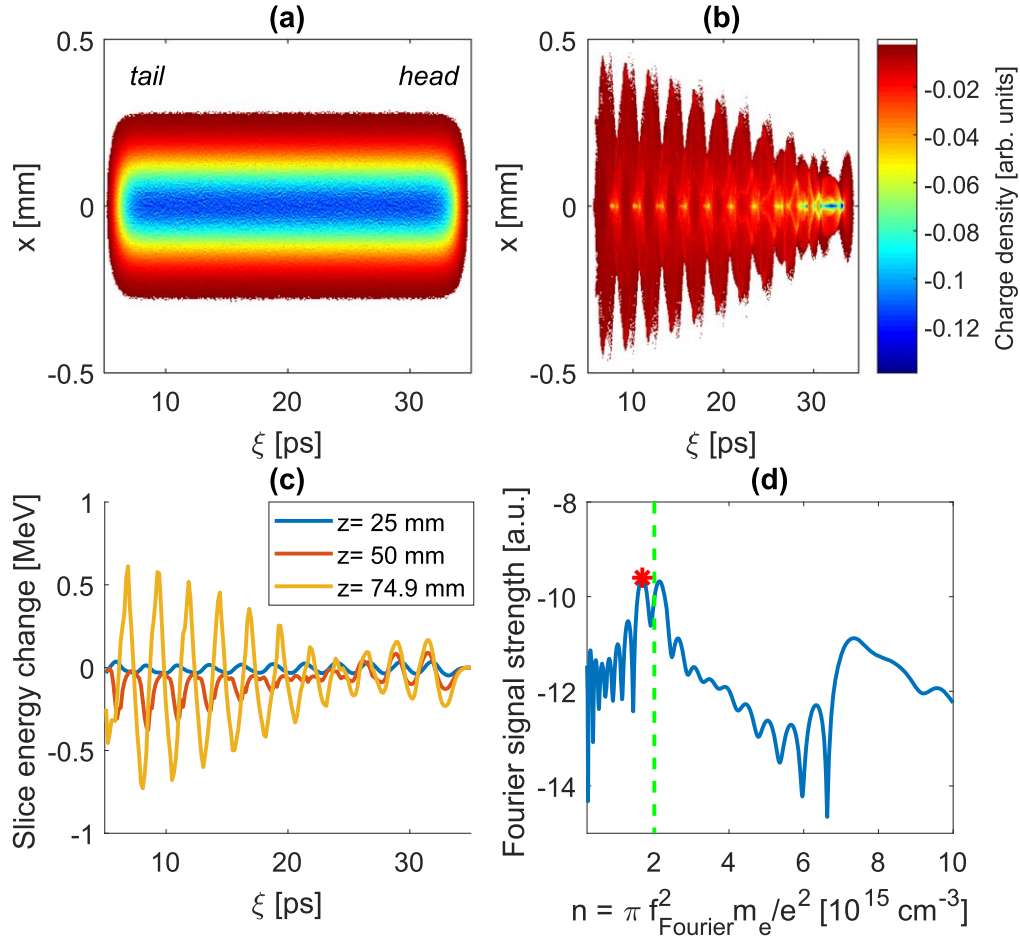


Figure 1. Simulated projections of a 530 pC bunch before the $2 \times 10^{15} \text{ cm}^{-3}$ plasma (a) and after 50 mm of propagation (b) in the x - ξ plane [$\xi = (z-ct)/c$] in linear color scale. Slice energy changes due to the driven wakefields at different positions in the plasma are depicted in (c). (d) shows the Fourier spectrum after 50 mm propagation in the plasma, where Fourier frequencies have been converted to plasma densities n according to equation (1). The green line indicates the simulated plasma density and the red star indicates the density that would be measured with the presented method.

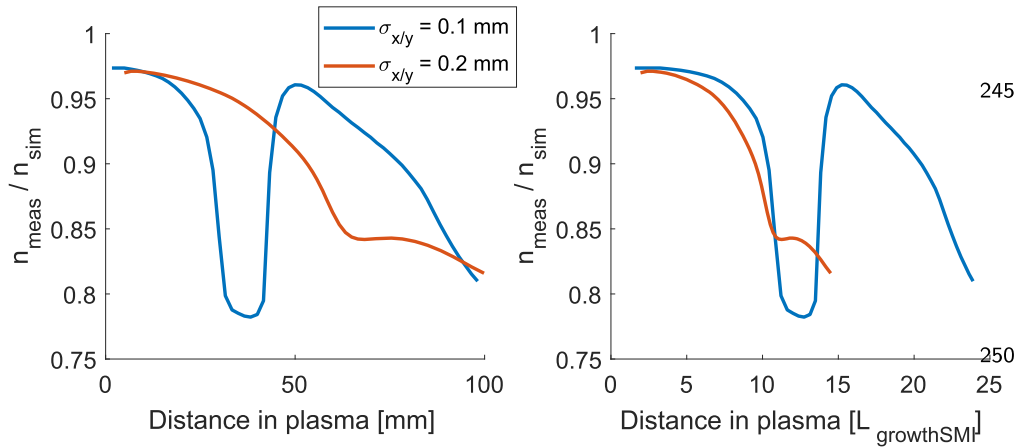


Figure 2. Simulated evolution of the (ideal) measurement accuracy along the plasma for two different probe bunches, with 510 pC, 27 ps FWHM length at a plasma density of $0.5 \times 10^{15} \text{ cm}^{-3}$. The transverse RMS-size $\sigma_{x/y}$ of the bunches at the entrance into the plasma was varied and the curves are shown for geometrical distances (left) and measured in SMI growth lengths (right).

experiments was simulated to be $\pm 5\%$. These values are therefore considered for the measurement results below, in case no individual simulation of a measurement was performed.

4. Beam-based density measurement

The SMI-based density measurements were performed at the PITZ facility using the available LPS-diagnostics [13, 23–25].

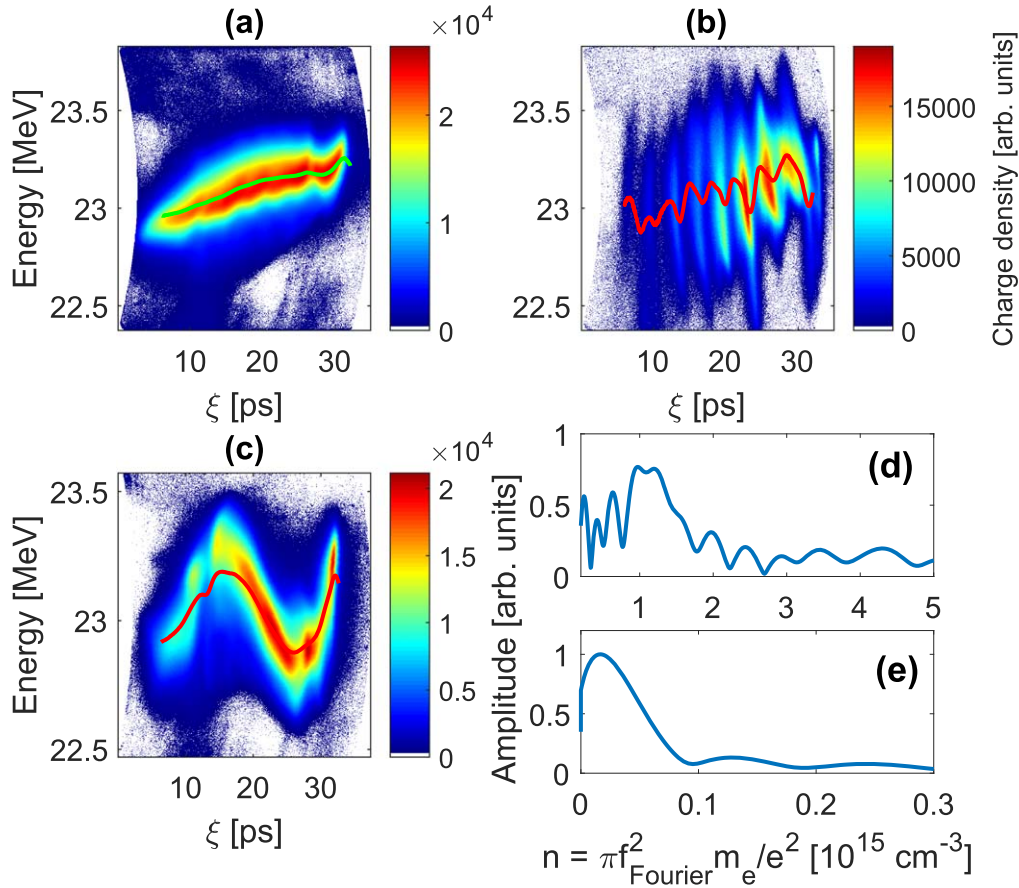


Figure 3. Non-interacting (a) and self-modulated electron beams (b), (c) with indicated mean slice energy ((a) green line; (b), (c) red lines) in linear color scale. The Fourier spectra for the two modulated beams are shown at high plasma density (d) ($45 \mu\text{s}$ delay to discharge ignition, corresponding to (b)) and low plasma density (e) ($240 \mu\text{s}$ delay to discharge ignition, corresponding to (c)).

The 23 MeV electron bunches coming from the L-band photo-injector linac are vertically deflected in a 2.998 GHz TDS cavity and dispersed horizontally in a dipole spectrometer, both downstream of the plasma cell. Transverse projection of the bunch charge on a subsequent scintillator screen yields the bunch LPS, after beam-plasma interaction over the full plasma length. The plasma cell [21] consists of a central 100 mm long Quartz-glass tube with an inner diameter of 10 mm. A voltage pulse of 2.4 kV is applied between the electrodes at the ends of the glass tube. The 0.6 mbar argon gas in the cell is heated and ionized by a 330 A peak current pulse of ca. $2 \mu\text{s}$ length.

Figure 3 shows the measured LPS for flat-top electron bunches without (a) and with (b), (c) interaction with the argon discharge plasma for different beam delays with respect to discharge initiation. The figures represent an average of 10 subsequent measurements of the transverse bunch distribution downstream the transverse deflector and the dipole spectrometer, from which the background signal has been subtracted and which have been corrected for chromaticity. It can be seen that the modulation period is changing significantly from high densities (b) to low densities (c). The drop in density with increasing beam-plasma delay corresponds to the recombination of plasma electrons and ions. The Fourier spectrum (with frequencies converted to corresponding plasma densities) at low density (figure 3(e)) shows a clear

peak at $2 \times 10^{13} \text{ cm}^{-3}$ and low amplitude side bands. At high plasma densities (figure 3(d)) determination of the plasma density is more complex: the appearance of a peak at $1.2 \times 10^{15} \text{ cm}^{-3}$, slightly higher than the density at the highest signal (ca. $1 \times 10^{15} \text{ cm}^{-3}$), can be seen. This effect was found in the simulations for cases in which the energy modulation is evolving after the transition of phase velocity during self-modulation, which corresponds to the development stage shown in figure 1(d). The assumption that the simulated case is similar to the measurement is supported by the fact that the measured LPS in figure 3(b) does not show significant growth towards the tail of the bunch, which is similarly found in figure 1(c), $z = 50 \text{ mm}$. Therefore, the peak at $\sim 1.2 \times 10^{15} \text{ cm}^{-3}$ is assumed to be closer to the actual plasma density in this case. Simulation of the individual case supports such a decision.

Plasma densities measured with the presented method are shown in figure 4. The maximum simulated measurement errors are included in the error bars. Further errors are mainly caused by bunch length measurement uncertainties. Bunch lengths are measured by scanning the RF phase of the bunch in the TDS cavity and comparing the known RF phase step length with the transverse offset caused by the phase step to the bunch projection on the measurement screen. Errors introduced by bunch length measurement uncertainties were

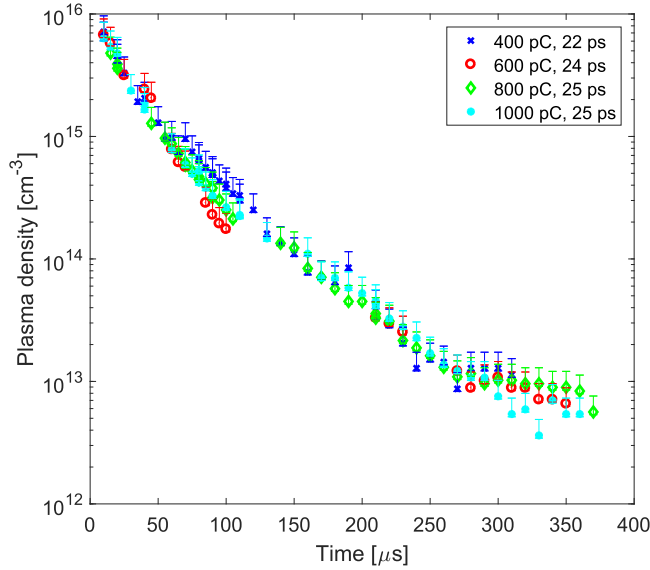


Figure 4. Plasma densities measured with probe beams of different total charge and correspondingly varying bunch length. The delay after triggering the discharge in the plasma source is varied to observe the density evolution.

found to be on the order of 1% and hence significantly smaller than simulated errors. Therefore, the measurement error can be reduced significantly by simulating individual interaction cases, as stated above.

5. Comparison to spectroscopic measurements

The density of the used gas discharge plasma cell was also measured using established spectroscopic methods. Hydrogen line profiles were measured and the line broadening due to the Stark-effect by free plasma electrons was used to deduce the density according to two commonly used references of semi-analytical and simulated Stark-broadening data by Griem [6] and Gigosos *et al* [7], respectively. 5% of hydrogen were added to the argon discharge gas to provide the Balmer- α line for the spectroscopic analysis as it exhibits high signal strength, substantial Stark-broadening and a profound basis of theoretical and experimental Stark-broadening data. The influence of the low percentage of hydrogen on the discharge dynamics is assumed to be negligible. Measurements were done using a Sopra UHRS F1500DP Fastie-Ebert configuration spectrometer with an Echelle grating operated in the 8th diffraction order and an ICCD camera with an overall spectral resolution of 3 pm at 656 nm. The plasma light emitted from the longitudinal and vertical center of the discharge vessel was collected with an optical fiber, which transported the light to the entrance of the spectrometer. Instrumental and Doppler-broadening was deconvoluted from the measured line profiles and a Lorentz-curve fit was used to evaluate the half width at half maximum. The plasma electron temperature was calculated numerically to be around 1 eV [21, 26]. LPS measurements for bunches interacting with the plasma during the discharge current pulse were not considered due to the unknown effect of magnetic fields induced by this current. The density results can be seen in

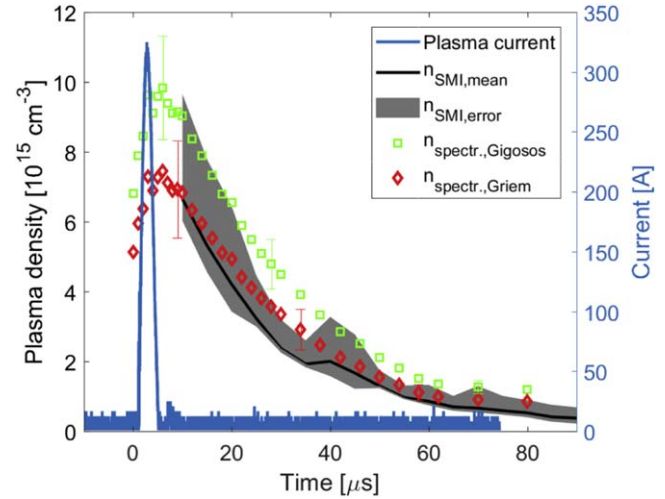


Figure 5. Current in the plasma source discharge and plasma densities n , measured with spectroscopic and SMI-based methods in the first 90 μs after discharge ignition. Densities measured by SMI were averaged for measurements with different bunch parameters (see also figure 4) and the extrema of the measurement errors are shown.

figure 5. Exemplary errors for the spectroscopic measurements include temperature uncertainties as well as methodical errors. The error of the SMI-based measurements shows the maximally and minimally measured densities including errors for the different measurements shown in figure 4.

Reasonable agreement is found between densities measured with the different methods. Spectroscopic measurement accuracy could be increased by measuring the time-resolved plasma temperature, which might also improve agreement between the measurements. Nevertheless, due to low light emission and small line broadening at low densities the spectroscopic measurements could only be used to measure the density in the beginning (ca. 0–90 μs) of the discharge. By using the SMI-based method, the measurement range could be extended down to densities of several 10^{12} cm^{-3} at delays of more than 350 μs after the discharge ignition, as shown in figure 4. The agreement of the measurements also suggests reasonable transverse homogeneity of the gas discharge plasma, as the emitted light that is used for the spectroscopic density measurement is integrated over the whole transverse size of the discharge vessel.

6. Conclusion

In summary, a new method to measure the plasma electron density based on the self-modulation of a relativistic electron bunch is presented. The measurement accuracy was evaluated by means of simulations and reference measurements using established spectroscopic plasma density measurement methods. This allowed to define the error range of SMI-based density measurement, which has not been determined in previous work [13]. According to these results, the measurement error can be as low as a few percent, depending on the exact bunch/plasma parameters. The method is independent of the ion species of the plasma and has already been used for

argon gas discharge and laser ionized lithium vapor plasmas. Necessary tools for application of the method primarily include high brightness probe particle bunches and diagnostics of the LPS of the latter (e.g. a spectrometer and a transverse deflecting cavity). Even though the measurement method is suitable for any laboratory plasma, the application is especially interesting for the plasma sources of PWFA facilities, where the necessary tools are naturally available [27–29]. Any density range with plasma wavelengths shorter or on the order of the maximum available bunch length is accessible and densities between a few 10^{12} cm^{-3} and nearly 10^{16} cm^{-3} have been measured in experiments. This measurement range is defined by the available bunch diagnostics and therefore naturally adjusts to the range of interest of a PWFA experiment with the necessary LPS measurement tools. The method allows *in situ* density measurement of a mounted plasma source, e.g. after change of components, gas exchange or other influences. Additionally, the density is measured at the exact timing and transverse position of beam passage, while this has to be measured separately for density measurements with e.g. spectroscopic methods. Nevertheless, complimentary measurements with spectroscopic methods would also allow longitudinal resolution of the plasma density profiles, which is not achievable with the presented method due to the integration of energy changes to the beam particles along the plasma. The time resolution of the measurements corresponds to the transit time of the beam through the plasma $\tau = L_{\text{plasma}}/c$ and therefore allows sub-ns resolution for cm-scale plasmas.

The method already enabled determination of plasma densities that were not accessible by spectroscopic methods due to low signal and signature strengths [23]. Also previously reported estimations of plasma densities by manual evaluation of the self-modulation periodicity [13, 30] have been significantly extended to lower densities by the proposed method. To further improve the measurement accuracy, calculation of the plasma length from the LPS of the probe bunch is under investigation, which would allow the thermal expansion of the plasma to be monitored.

Acknowledgments

The authors would like to thank T Mehrling and A Martinez de la Ossa for useful discussions on the particle-in-cell simulations, as well as A Yeremyan, A Vardanyan and other colleagues from CANDLE, Yerevan, Armenia for their great support in operating the PITZ facility and the DESY technical staff for their assistance with the experimental work.

ORCID iDs

G Loisch  <https://orcid.org/0000-0002-6178-2339>

G Asova  <https://orcid.org/0000-0002-9724-5447>

P Boonpomprasert  <https://orcid.org/0000-0001-9831-1410>

Y Chen  <https://orcid.org/0000-0003-1318-5561>

J Good  <https://orcid.org/0000-0002-6960-5345>

M Gross  <https://orcid.org/0000-0002-4457-8897>

M Krasilnikov  <https://orcid.org/0000-0002-1278-4426>

O Lishilin  <https://orcid.org/0000-0002-7286-599X>

A Oppelt  <https://orcid.org/0000-0001-5547-7402>

H Qian  <https://orcid.org/0000-0002-3213-0892>

F Stephan  <https://orcid.org/0000-0001-5654-1250>

References

- [1] Tajima T and Dawson J M 1979 *Phys. Rev. Lett.* **43** 267–70
- [2] Chen P, Dawson J M, Huff R W and Katsouleas T 1985 *Phys. Rev. Lett.* **54** 693–6
- [3] Malka V *et al* 2002 *Science* **298** 1596–9
- [4] Esarey E, Schroeder C B and Leemans W P 2009 *Rev. Mod. Phys.* **81** 1229–86
- [5] Blumenfeld I *et al* 2007 *Nature* **445** 741–4
- [6] Griem H R 1964 *Principles of Plasma Spectroscopy* (Maryland: McGraw-Hill Book Company)
- [7] Gigos M A, González Á and Cardeñoso V 2003 *Spectrochim. Acta B* **58** 1489–504
- [8] Muggli P, Marsh K A, Wang S, Clayton C E, Lee S, Katsouleas T C and Joshi C 1999 *IEEE Trans. Plasma Sci.* **27** 791–9
- [9] Lotov K V 1998 *Nucl. Instrum. Methods Phys. Res. A* **410** 461–8
- [10] Kumar N, Pukhov A and Lotov K 2010 *Phys. Rev. Lett.* **104** 255003
- [11] Schroeder C B, Benedetti C, Esarey E, Grüner F J and Leemans W P 2011 *Phys. Rev. Lett.* **107** 145002
- [12] Schroeder C B, Benedetti C, Esarey E, Grüner F J and Leemans W P 2013 *Phys. Plasmas* **20** 056704
- [13] Gross M *et al* 2018 *Phys. Rev. Lett.* **120** 144802
- [14] Adli E *et al* 2018 *Nature* **561** 363–7
- [15] Tonks L and Langmuir I 1929 *Phys. Rev.* **33** 195–210
- [16] Emma P, Frisch J and Krejcik P 2000 A transverse RF decting structure for bunch length and phase space diagnostics *Tech. Rep. LCC - 0047 and LCLS-TN-00-12* Stanford Linear Accelerator Center SLAC
- [17] Krasilnikov M *et al* 2012 *Phys. Rev. Spec. Top. - Acc. Beams* **15** 100701
- [18] Mehrling T, Benedetti C, Schroeder C B and Osterhoff J 2014 *Plasma Phys. Control. Fusion* **56** 084012
- [19] Will I and Klemz G 2008 *Opt. Express* **16** 14922–37
- [20] Loisch G *et al* 2018 *Nucl. Instrum. Methods Phys. Res. A* **909** 107–10
- [21] Loisch G *et al* 2019 *J. Appl. Phys.* **125** 063301
- [22] Mehrling T J, Fonseca R A, Martinez de la Ossa A and Vieira J 2017 *Phys. Rev. Lett.* **118** 174801
- [23] Loisch G *et al* 2018 *Phys. Rev. Lett.* **121** 064801
- [24] Kravchuk L *et al* 2010 Layout of the PITZ transverse deflecting system for longitudinal phase space and slice emittance measurements *Proc. 25th Lin. Acc. Conf.* (Geneva: JACoW) pp 416–8
- [25] Huck I *et al* 2015 First results of commissioning of the PITZ transverse deflecting structure *Proc. 37th Int. FEL Conf.* (Geneva: JACoW) pp 110–4
- [26] Anania M P *et al* 2016 *Nucl. Instrum. Methods Phys. Res. A* **829** 254–9
- [27] Aschikhin A *et al* 2016 *Nucl. Instrum. Methods Phys. Res. A* **806** 175–83
- [28] Rossi A R *et al* 2014 *Nucl. Instrum. Methods Phys. Res. A* **740** 60–6
- [29] Dorda U *et al* 2016 *Nucl. Instrum. Methods Phys. Res. A* **829** 233–6
- [30] Gross M *et al* 2018 Characterization of self-modulated electron bunches in an argon plasma *J. Phys.: Conf. Ser.* **1067** 042012